

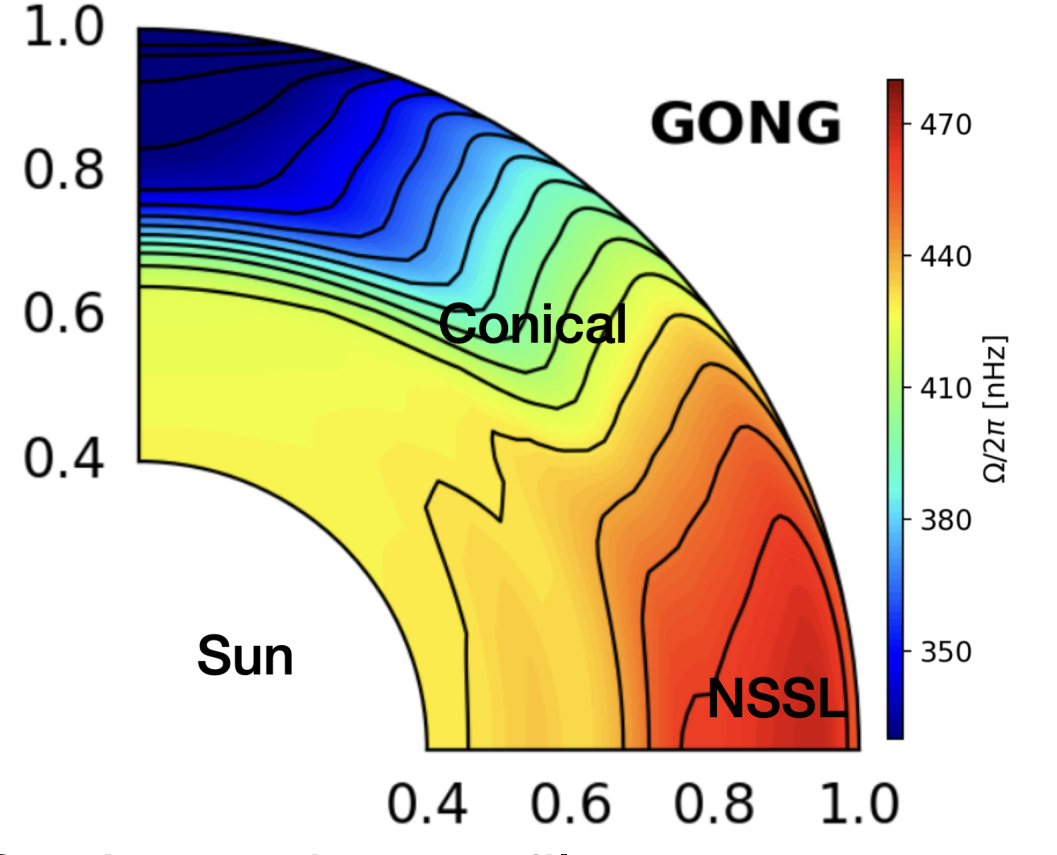
Aims

1. Unveiling the rotation profile during the transition from a (SL) to an (AS) rotation profile at the end of the low mass star Main Sequence (MS).
2. How the heat is it transported before, during and after the transition?

0. Introduction

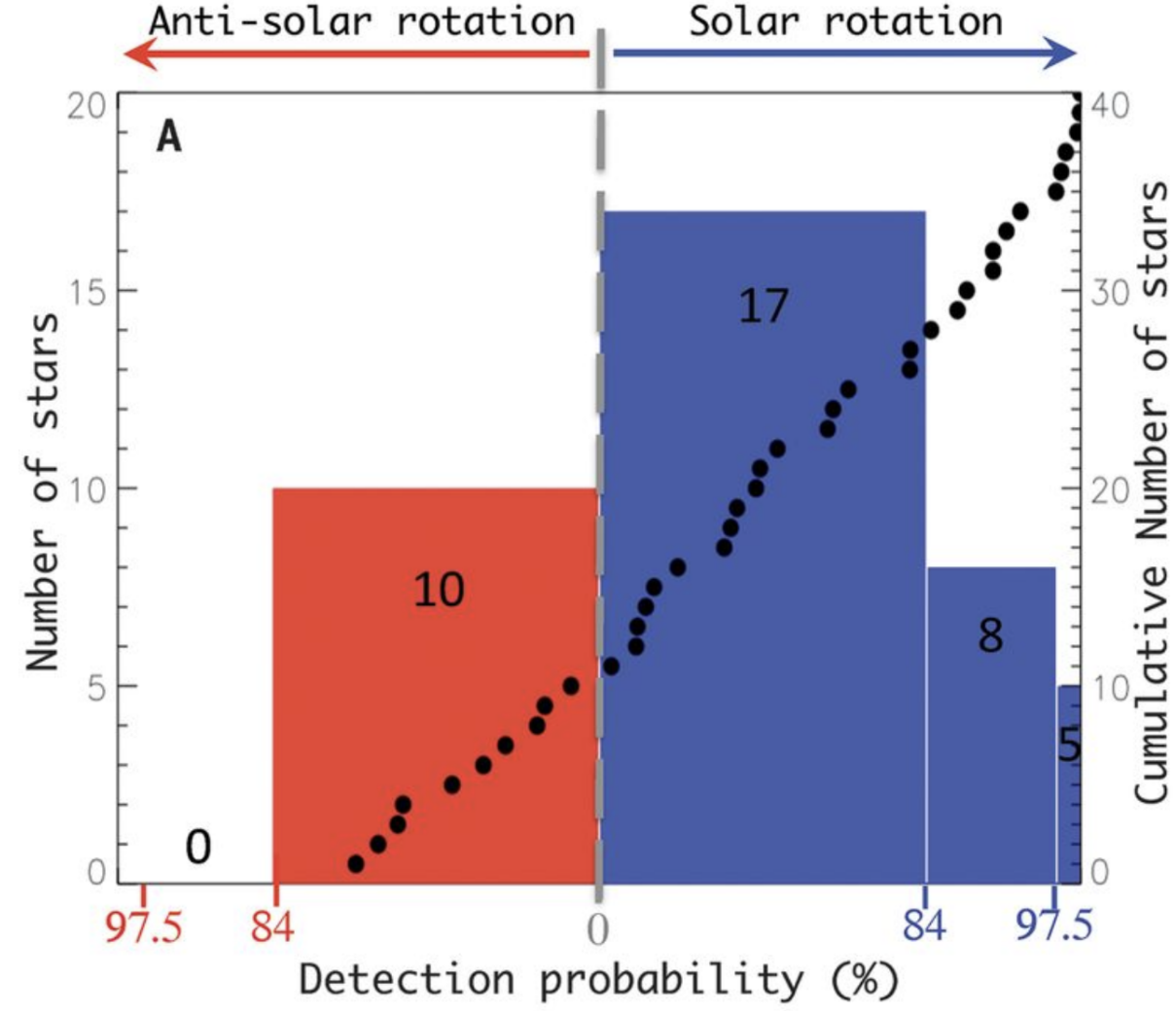
2 rotation profiles observed/expected for the low mass stars :

Solar-Like(SL): equator rotates faster than the poles; **Observed**

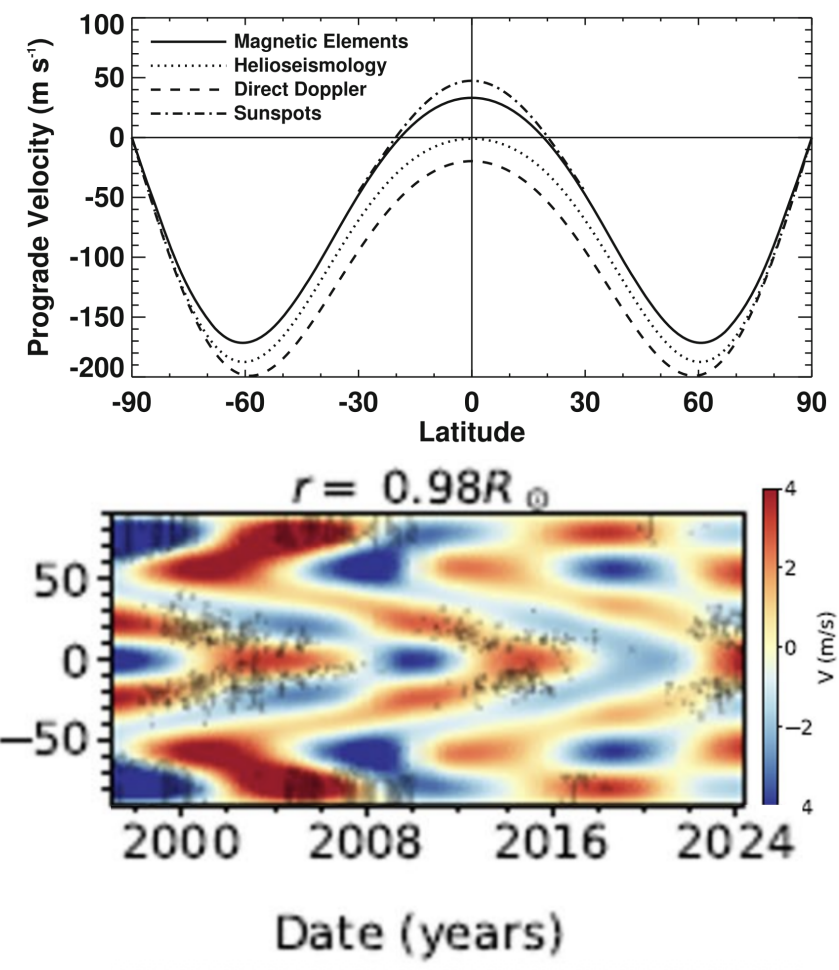


Sun's rotation profile adapted from [1]

Anti-Solar(AS): equator rotates slower than the poles; **Not observed yet with certainty**



(SL) & (AS) detection probability [2]

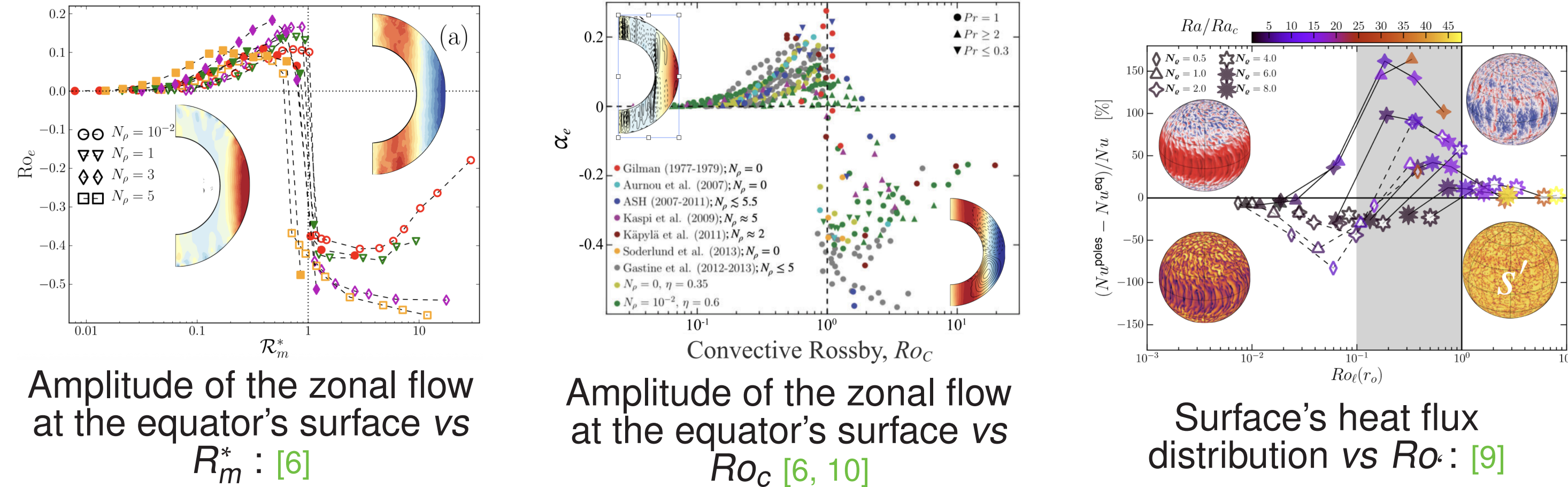


Sun's surface rotation profile and Torsional Oscillations (TO) [4, 5]

2 questions still in debate in stellar physics [1]:

- Reproduce the conical shape of the rotation at mid-latitude in the 3D numerical simulations
- Reproduce the Near Sub-surface Shear Layer (NSSL) in the 3D numerical simulations

The convective Rossby number Ro_c , modified Rayleigh R_m^* and local Rossby numbers Ro , control the transition (SL)-(AS) rotation and the heat transport [6, 7, 8, 9, 10]:



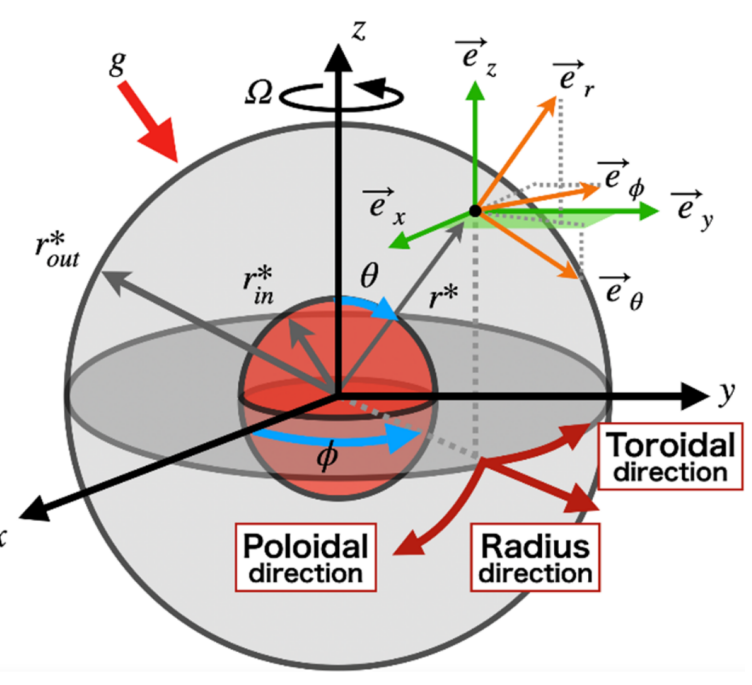
Limits:

- the parameter space is far removed from the stellar values: lower Pr and/or higher density contrast imposed N_p
- Ro_c does not explain the sharp transition for the transition (SL)-(AS) profiles
- the (NSSL) does not seem to appear in these simulations

I. Star considered, its numerical model [9] and equations [11]

Low mass star:= Radiative core (ignored) and convective envelope:

- Young red giant stars with a thick convective shell ($r \in [0.35, 1]r_o$)



Extracted from [13]

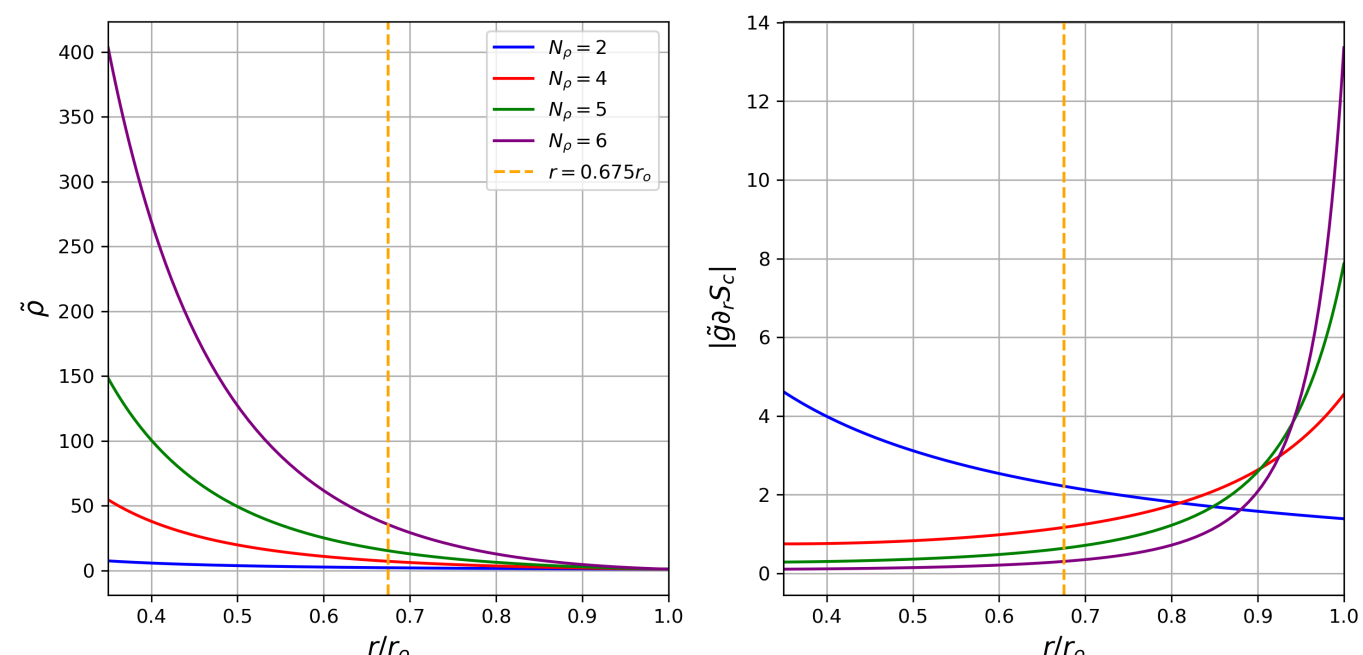
Navier-Stokes, mass, energy equations in the hydro. anelastic approximation:

- Navier-Stokes:
- Where S is the Strain tensor
- Mass conservation:

$$\frac{Dv}{Dt} = -\frac{1}{E_k} \nabla \left(\frac{P'}{\rho} \right) - 2 \frac{1}{E_k} \Omega \wedge v - \frac{Ra}{Pr} S'g + \frac{1}{\rho} \nabla \cdot S$$

- Energy (Entropy form):
- Where Q_v is the viscous heating
- Adiabatic reference state

Characteristic values in the (CZ):			
Parameter	Ratio	IRL.	Simu.
Prandtl	$Pr = \frac{\nu}{\kappa}$	10^{-5}	0.1
Rayleigh	$Ra = \frac{G \Delta S d^3}{C_p \nu \kappa}$	10^{30}	$10^5 - 10^7$
Ekman	$E_k = \frac{\nu}{\Omega d^2}$	10^{-15}	$3 \cdot 10^{-4}$
Density contrast	$N_p = \log(\bar{\rho}_i / \bar{\rho}_o)$	/	{2, 4, 5, 6}
Polytrop. index	n	/	2
Nusselt	$Nu = 1 + \frac{L_{conv}}{L_{rad}}$	/	/
Conv. Rossby	$Ro_c = \sqrt{\frac{Ra E^2}{Pr}}$	/	/
Ra mid-depth	$\sqrt{R_m^*} = Ro_c \sqrt{g \partial_r S'_c}$	/	/



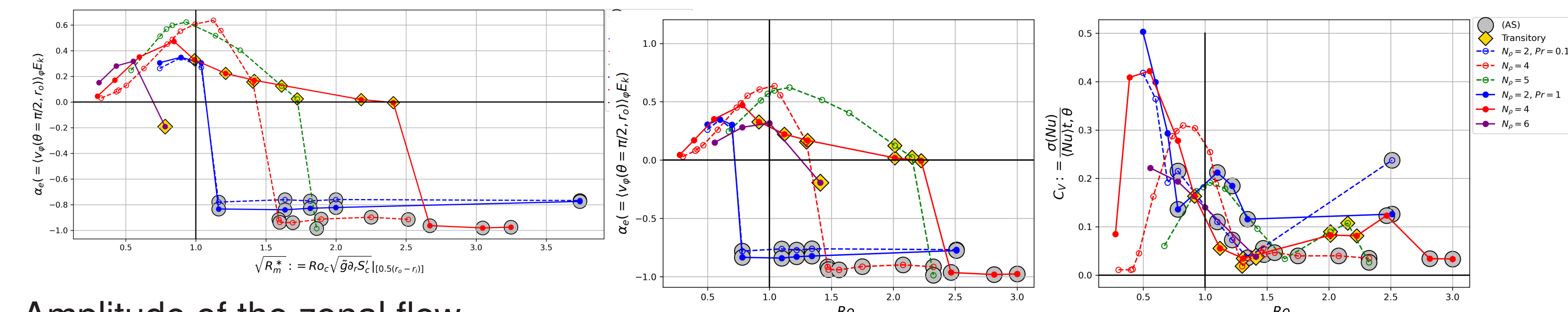
Adiabatic backgrounds for the density, the gravity and the conductive entropy (gradient)

Angular momentum equation:

$$\rho \frac{\partial(\mathcal{L})}{\partial t} = -\nabla \cdot (\mathcal{F}_{Mer}) + \nabla \cdot (\mathcal{F}_{Re} + \mathcal{F}_v) \quad (1)$$

$$\tilde{\rho} \langle v_m \rangle_\theta \cdot \nabla \mathcal{L} \approx -\nabla \cdot (\tilde{\rho} \sin(\theta) \langle u' \cdot u'_\theta \rangle_\theta) \quad (2)$$

II. Towards stellar parameters show some limits of the previous studies



Amplitude of the zonal flow at the equator's surface vs $\sqrt{R_m^*}$

Amplitude of v_ϕ at the equator's surface & the surface's heat flux vs Ro_c

- Reproduction of the 2 rotation profiles as in the literature: a (SL) rotation profile for $Ro_c < 1$ and an (AS) one for $Ro_c > 1$... **But**
- The Pr (intrinsic properties of the fluid) and the density contrast delay the transition from a (SL) to an (AS) rotation profile even at $Pr = 1 \Rightarrow$ The Ro_c and R_m^* which are independent of the diffusivities do not catch properly the transition.
- The coefficient of variation of the axisymmetric heat flux $C_v = \sigma(Nu) / \langle Nu \rangle_{t,\phi}$ shows the same trend when the $Ro_c \nearrow$

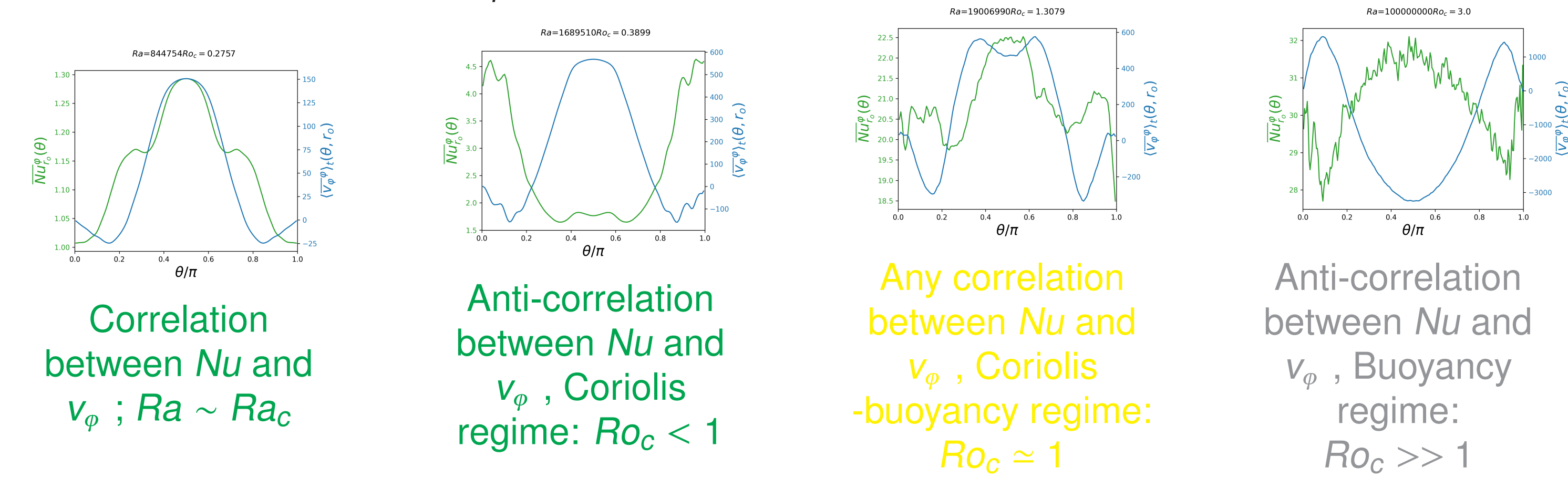
► The simulations with a high N_p at $Ro_c \approx 1$ are in transition and present 2 new rotation profiles

3 different regimes for the heat flux distribution at the surface: Uniform (U), Poles hotter than the equator (PH), Equator hotter than the poles (EH):

$$(U) / (EH) \xrightarrow{Ro_c \nearrow} (PH) \xrightarrow{Ro_c \nearrow} (U) \xrightarrow{Ro_c \nearrow} (EH) \xrightarrow{Ro_c \nearrow} (U) \xrightarrow{Ro_c \nearrow} (PH)$$

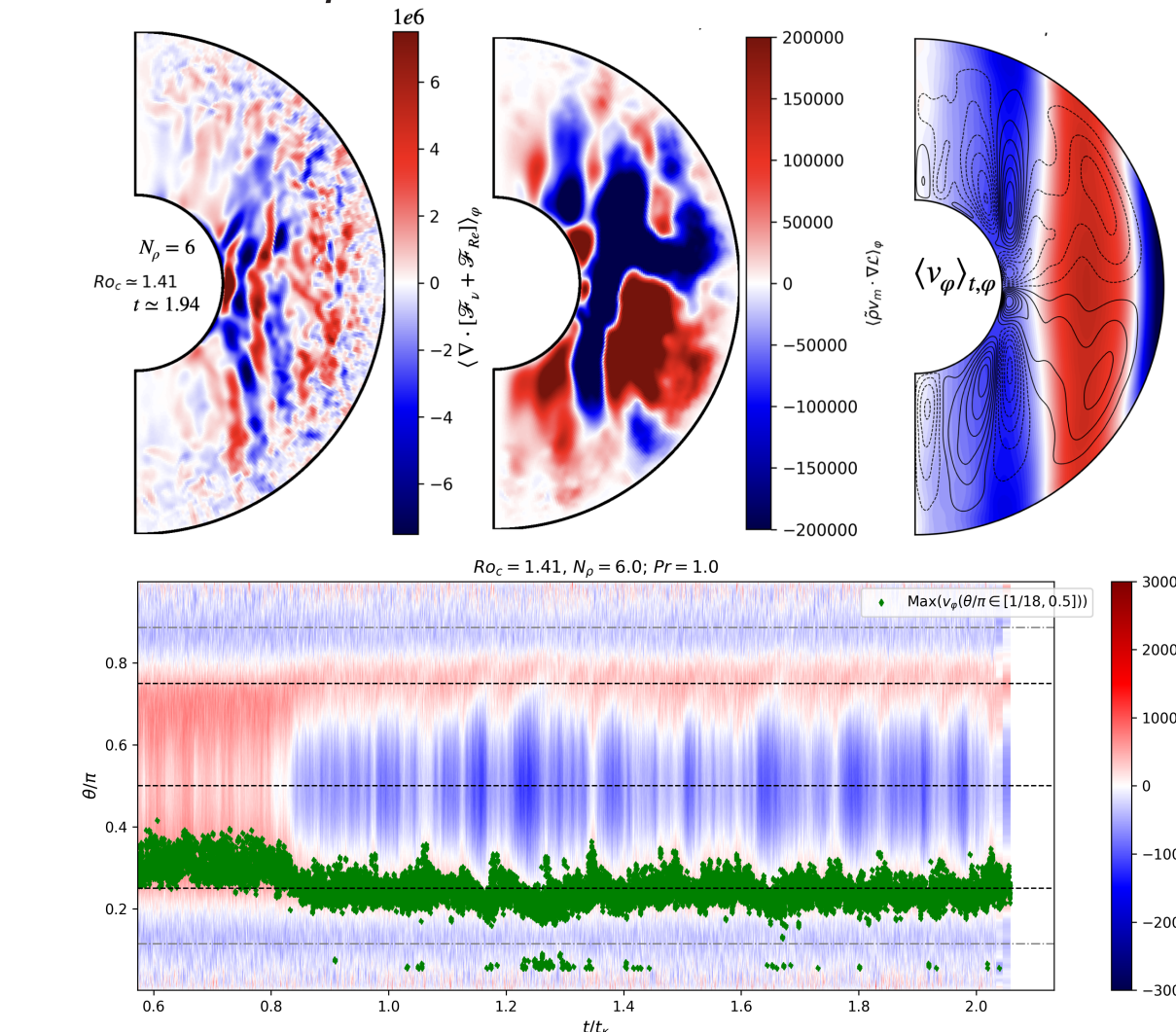
The 2 last regimes are reached only at $N_p = 2$ due to the high level of turbulences.

Examples of the results for $N_p = 4, Pr = 1$:



III. 2 new rotation profiles at $Ro_c \approx 1$ and 1 new convective regime

I. (a) Toward the (NSSL) when a more realistic N_p is imposed ?

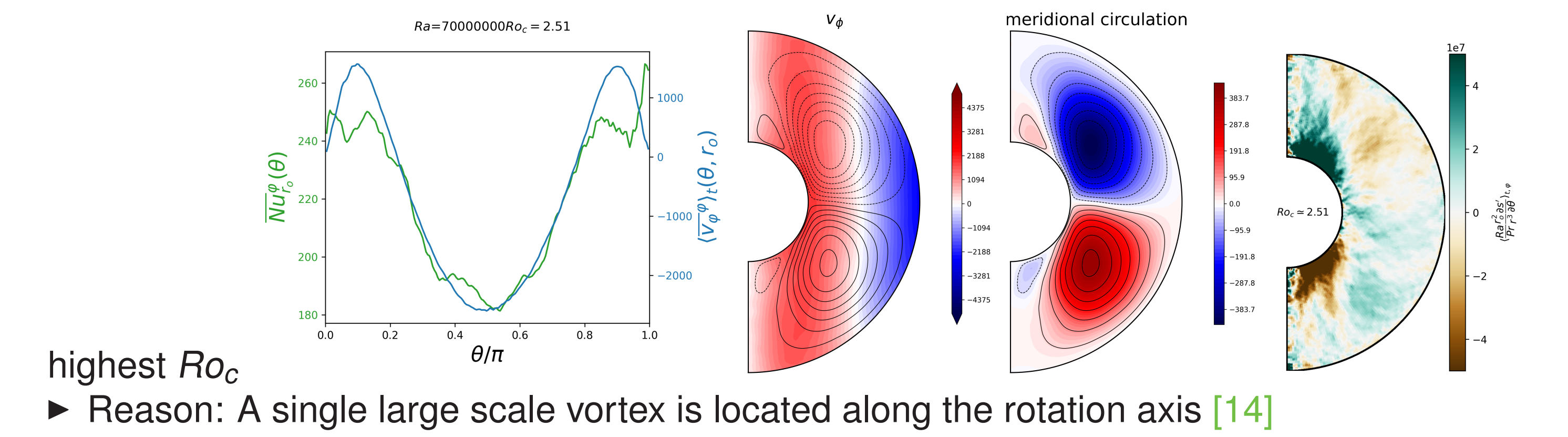


- 2 regimes coexist simultaneously: Coriolis within the tangent cylinder and the buoyancy outside the (TC)
- the system is balanced between the meridional circulation and the Reynolds stress at mid-depth in a steady state

Thermal wind equation :

$$\frac{\partial \langle u_\phi \rangle_\phi}{\partial z} \approx \frac{Ra^2 \partial \langle s' \rangle_\phi}{Pr r^3 \partial \theta} \quad (3)$$

II. A new convective regime: a correlation between the Nu and v_ϕ in an (AS) regime for the



highest Ro_c

- Reason: A single large scale vortex is located along the rotation axis [14]

Conclusions / Perspectives

1. We have seen the limits of the Ro_c for the transition (SL)-(AS), and we want to improve this prescription by finding another parameter and explain the 2 new rotation regimes.
2. By adding a radiative zone (RZ) below the (CZ) in order to be closer to the reality, we want to see if we will observe the conical shape of the rotation at mid-latitude in the (SL) and (AS) low mass stars as in [12]

References

[1] Hotta et al., Dynamics of large-scale solar flows. Space Science Reviews, 2023
 [2] Benomar et al., Asteroseismic detection of latitudinal differential rotation in 13 Sun-like stars. Science, 2018
 [3] Constantin et al., Stratospheric Planetary Flows from the Perspective of the Euler Equation on a Rotating Sphere. Springer, https://ui.adsabs.harvard.edu/abs/2022ArMA.245.587C, 2022
 [4] Hanasoge et al., Surface and interior meridional circulation in the Sun. Springer, https://doi.org/10.1007/s41116-022-00034-7, 2022
 [5] Mandal et al., Helioseismic evidence that the solar dynamo originates near the tachocline. Nature, 2026
 [6] Gastine et al., Effects of compressibility on driving zonal flow in gas giants. Icarus, 2012
 [7] Gastine et al., Zonal Flow Regimes in Rotating Anelastic Spherical Shells: An Application to Giant Planets. Icarus, 10.1016/j.icarus.2013.02.031, 2013
 [8] Gastine et al., From solar-like to antisolar differential rotation in cool stars. MNRAS, 2014
 [9] Raynaud et al., Gravity Darkening in Late-Type Stars. I. The Coriolis Effect. A&A, 10.1051/0004-6361/201731729, 2018
 [10] Soderlund et al., Magnetohydrodynamic control of differential rotation and dynamo transitions: rise of the local magnetic Rossby number. MNRAS, 2025
 [11] Jones et al., Anelastic Convection-Driven Dynamo Benchmarks. Icarus, 10.1016/j.icarus.2011.08.014, 2011
 [12] Brun et al., On Differential Rotation and Overshooting in Solar-like Stars. A&A, 2017
 [13] Satake et al., Influence of Centrifugal Buoyancy in Thermal Convection within a Rotating Spherical Shell. Symmetry, 10.3390/sym14102021, 2022
 [14] Lin et al., Large-scale vortices and zonal flows in spherical rotating convection. JFM, 2021